Connection of Planetary Waves in the Stratosphere and Ionosphere by the Modulation of Gravity Waves

P. Hoffmann, Ch. Jacobi

Abstract

A possible connection of planetary waves (PW) and ionospheric planetary wave type oscillations (PWTO) at midlatitudes is studied by analyzing MetOffice stratospheric reanalysis data and maps of the Total Electron Content. Although the seasonal variability looks similar, the vertical coupling between stratosphere and ionosphere is known to only happen indirectly through processes such as the modulation of gravity waves (GW) by PW. To investigate possible coupling processes, information about GW are retrieved from SABER temperature profiles (30-130 km) by calculating the potential energy (E_p) and generating daily maps of E_p. For the period of time from 2003-07-19 to 2005-07-20 proxies of stationary and travelling PW were calculated to obtain a general picture of PW activity, modulation of GW by PW and activity of PWTO in the ionosphere. The results reveals that mostly PW itself cannot reach lower thermospheric heights, but their signatures propagate upward up to 120 km and above, where they can trigger PWTO.

Zusammenfassung

Ein möglicher Zusammenhang zwischen dem Auftreten planetarer Wellen (PW) und typischer Oszillationen planetarer Wellen (PWTO) der Ionosphäre in mittleren Breiten wird auf der Basis von Analysen stratosphärischer Reanalysen und Karten des Gesamtelektronengehalts untersucht. Obwohl das saisonale Verhalten ähnlich erscheint, kann die Kopplung nur auf indirektem Wege erfolgen, wie z.B. durch die Modulation von Schwerewellen (GW) durch PW. Die für die Analysen notwendigen Informationen über GW können aus Temperaturprofilen (30-130 km), abgeleitet von Satellitenbeobachtungen (z.B. SABER), durch die Bestimmung der potentiellen Energie von GW, gewonnen werden. Zusammengefasst in täglichen Daten (2003-07-19 to 2005-07-20) stellen Proxies stationärer und wandernder PW ein vereinfachtes Bild des Prozesses der Modulation durch PW dar. Die Ergebnisse zeigen, dass sich PW selbst nicht bis in die unteren Thermosphäre ausbreiten können. Jedoch die Signatur, getragen durch GW, könnte auf diesem Wege als PWTO abgebildet werden.

1. Introduction

The variability of the ionosphere is mainly driven by regular and irregular variations of the extreme ultra-violet solar radiation (EUV) and the Earths magnetic field. However, planetary wave type oscillation (PWTO) having periods of several days have also been observed in ionospheric parameters (e.g. Total Electron Content and f_oF2), and show a similar seasonal behavior in comparison to stratospheric planetary waves (PW) at midlatitudes (Borries et al., 2007) and to the meridional neutral winds in the mesosphere/lower thermosphere (MLT) region (Altadill et al., 2003). Until now no clear evidence exist that such oscillations are forced by waves coming from the lower atmosphere. From theory and model experiments (e.g. Pogoreltsev et al., 2007) is known that stationary and long-period PW cannot propagate vertically into the lower thermosphere due to the critical layer filtering near the mesopause region and other processes such as diffusion. However, indirect coupling processes could exist, such as the modulation of GW by PW (e.g. Laštovička, 2006), which may transport signatures of PW from the stratosphere/mesosphere to the thermosphere.

Since 2002 a space-based temperature data set from the SABER instrument onboard the TIMED satellite is available, which covers the lower and midlatitudes (52°N to 52°S) from the stratosphere up to the lower thermosphere (130 km) without gaps. To extract information about GW from globally distributed temperature profiles one may calculate the potential energy (E_p) from these. Climatologies of GW E_p taken from satellite-borne temperatures are presented in e.g., Tsuda et al. (2000), Preusse et al. (2002), Preusse et al. (2006) and Fröhlich et al. (2007).

By calculating the potential energy of GW one may study the modulation by global scale waves such as PW in comparison to stratospheric PW and ionospheric PWTO. A detailed description of this method is given in section 2. The analysis of PW and the modulation of GW by PW is performed calculating proxies of PW in the space-time domain. Without any spectral decomposition we obtain a general picture of stationary and travelling components and their effects on GW amplitudes. The principle is given in section 3. However, in order to demonstrate a possible transmission path of vertical coupling through the modulation of GW, information about small scale Travelling Ionospheric Disturbances (TID) are essential. Their signatures over Europe can be retrieved from GPS signals as presented in Borries at al. (2009) and the data are used here to find the connection between TID and PWTO in comparison to stratospheric GW and PW.

Before studying the mechanism of coupling processes (in sections 5 and 6), a comparison of PW results obtained by MetOffice and SABER is presented in section 4, similar to Pancheva et al. (2009a), but using PW-proxies, to confirm the reliable picture of PW activity.

2. SABER data analysis

The TIMED satellite was launched on 7th of December 2001 into a 625 km orbit of 74.1° inclination to investigate the dynamics of the mesosphere, thermosphere and ionosphere. The SABER instrument on board of the spacecraft began making observations in late January 2002. By step-scanning the atmospheric limb SABER measures height profiles

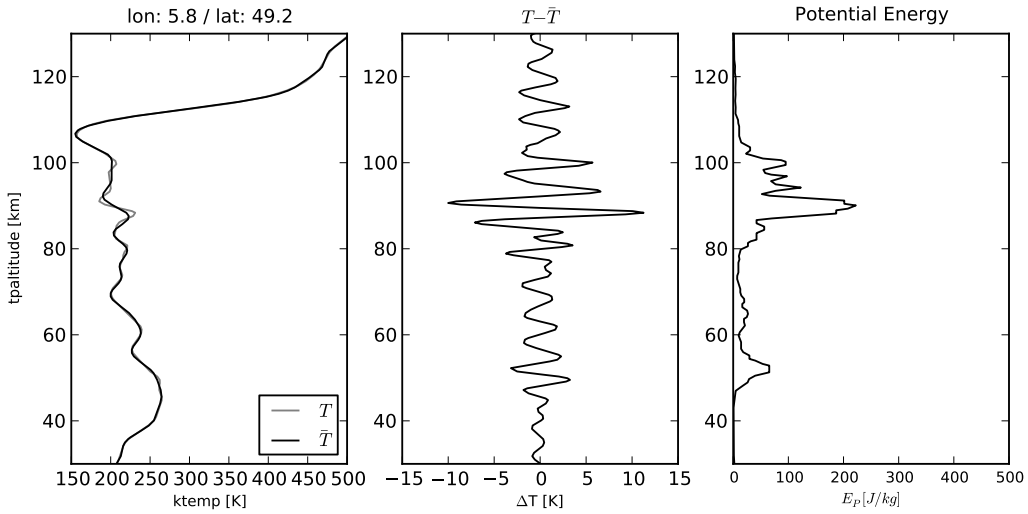

Figure 1: *Example of potential energy calculation (2003-12-12, 49.2°N, 5.8°E). Left panel: SABER temperature profile (T, grey line) and lowpass ($\lambda_z > 6\,km$) filtered profile ($\overline{T}$, black line). Middle panel: Residuals T'. Lower panel: potential energy E_p after Eq.1.*

of temperatures and selected chemical species from 10-180 km altitude with a horizontal resolution along track of about 400 km. The multispectral radiometer operates in the near to mid-infrared over the range 1.27 µm to 17 µm (7865 cm^{-1} to 650 cm^{-1}). It measures CO_2 infrared limb radiance from approximately 20-120 km altitude and the kinetic temperature profiles are retrieved over this heights using a full non-LTE inversion (Mertens et al., 2004). The used SABER L2A data (version 1.07) were downloaded from the web site: *http://saber.gats-inc.com*.

The SABER latitude coverage extends from about 52° of one hemisphere to 83° of the other. This latitude range is reversed by a yaw manoeuvre every 60-days. Due to the sun-synchronous orbital geometry the spacecraft passes the equator always at the same local time (12LT) on the dayside. Before collecting the observations of one day and adapting the orbital data to a regular 3D-grid, all geolocation information, temperature profiles (T) and the geometric height were extracted from the L2A product files and separated into ascending (T_{asc}) and descending (T_{dsc}) overflights (Oberheide et al., 2003). Thereby, the disturbing impact of the diurnal migrating tide can be reduced. Each single profile (Fig.1, left panel) having a vertical resolution of $\Delta z = 0.5\,km$ between 30-130 km is decomposed into harmonics (sine and cosine functions with $\lambda_z < 6\,km$) using the least-squares fit and reconstructed combining all harmonics having a vertical wavelength ($\lambda_z > 6\,km$) to obtain a filtered temperature profile $\bar{T}(z)$. As shown on Figure 1 (middle panel), the residual profile $T'(z)$ between the original $T(z)$ and the filtered profile $\bar{T}(z)$ reveals the vertical structure of GW amplitudes and their specific potential energy (right panel):

$$E_p = \frac{1}{2}\left(\frac{g}{N}\right)^2 \left(\frac{T'}{\bar{T}}\right)^2; \qquad (1)$$

whereas g and N represents the acceleration due to gravity and the Brunt-Vaisala frequency. This method is also used in e.g. Fröhlich et al. (2007) to extract GW energy

in the lower stratosphere from GPS radio occultation measurements. The spatial and temporal variations of the total energy integrated over a sliding vertical column (10 km) is used to study the modulation of GW. Note that the limb-scanning of the atmosphere by instruments satellites (e.g. SABER on TIMED) only certain parts of the GW spectrum is visible due to the integration along the line of sight (Preusse et al., 2006). Information about the horizontal wavelength vector, in particular perpendicular to the spacecraft orbit, are difficult to detect and only part of the GW energy is visible depending on horizontal resolution and viewing geometry with respect to the wavenumber vector.

A daily regular gridded picture for several parameters (T_{asc}, T_{dsc}, E_p) is obtained by median averaging all observations lying within a 3D-grid ($\Delta\lambda = 10°$, $\Delta\varphi = 5°$, $\Delta z = 2\,km$) covering the region from 45°S to 45°N between 30-130 km. Possible outliers getting less weight which reduces the day to day variation of the retrieved values and the data quality of the GW potential energy. A more technical description of this regularization using the programming language Python is given in Hoffmann et al. (2009). Due to the orbital geometry alising effects occur especially for analysing tidal waves in the mesosphere/lower thermosphere (MLT) region, and short-period PW.

The daily products of this procedure are depicted on Figure 2 for 45°N from the 2003-07-19 to 2005-07-20. The upper panel shows the daily zonal standard deviations

$$\sigma_x \{T_{dsc}\} = \sqrt{\frac{1}{nx} \sum_{\lambda} (T_{dsc} - \bar{T}_{dsc})^2} \tag{2}$$

as an approximation of PW activity, with nx being the number of data points in the zonal direction and λ is longitude. Below 80 km, the picture indicates the well known seasonal cycle of PW activity, with a maximum during winter. Above 80 km, the structures are somewhat questionable due to alising effects caused by tidal waves, which are subharmonics of the solar day composed into migrating and non-migrating components. Those amplitudes increase with altitude. The zonal mean $m_x \{T_{dsc}\} = \frac{1}{nx} \sum_{\lambda} T_{dsc}$ given in Figure 2 (middle panel) illustrates the background thermal structure of the middle atmosphere and its seasonal behavior. The lower panel in Figure 2 shows the daily zonal standard deviation of the GW potential energy $\sigma_x \{E_p\}$ (similar to Eq.2) as an approximation of modulation effects. The daily values predominately maximize, according to the increase of potential energy with altitude, in the mesopause region near 90 km, where GW become unstable, break and deposit momentum to the background flow leading to the background wind reversal. For the vertical propagation of PW this region acts like a barrier, only fast PW some GW are able to penetrate the lower thermosphere. Below 80 km a seasonal cycle similar to those of PW appears. Thus, information about the indirectly vertical propagating of PW can be retrieved by analyzing the modulation of GW. The signals of GW separated from PW and tides, which having typically greater vertical wavelength, are minor influenced by alising effects and can deliver a clearer picture of the vertical coupling process.

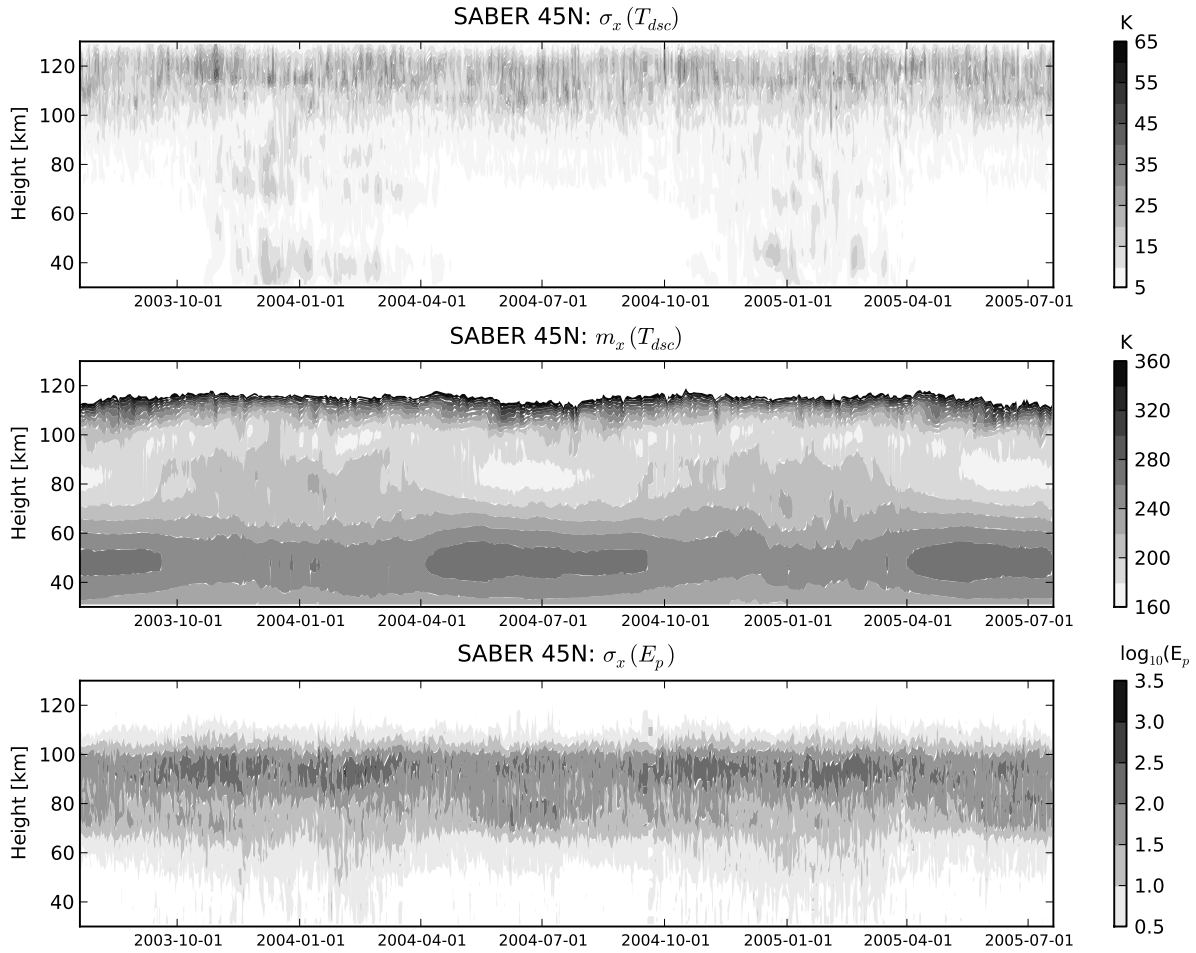

Figure 2: *Height-time cross-sections of SABER data at 45°N. Shown are daily zonal standard deviations ($\sigma_x\{T_{dsc}\}$, upper panel), daily zonal means ($m_x\{T_{dsc}\}$, middle panel) and daily zonal standard deviations of the potential energy ($\sigma_x\{E_p\}$, lower panle).*

3. Proxies of Planetary Waves

The space-time spectral analysis of PW first presented in Hayashi (1971) or PWTO at one latitude circle delivers a large number of wave components which are difficult to interpret. Thus, proxies of PW are introduced combining mean (m) and standard deviation (σ) in the longitude- (x) time (t) domain to study the problem of vertical coupling by the modulation of GW to obtain a general picture of such mechanism. Thereby, we simply differ between a proxy for stationary waves

$$\sigma_x(m_t\{A\}) = \sqrt{\frac{1}{nx-1}\sum_{\lambda}\left(\left\{\frac{1}{nt}\sum_{t}A(t,x)\right\} - \overline{\left\{\frac{1}{nt}\sum_{t}A(t,x)\right\}}\right)^2}, \qquad (3)$$

with A as the parameter under investigation, such as (T_{1hPa}, T_{dsc}, E_p), and a proxy for travelling waves defined as the difference between a proxy including all propagating components

$$m_x(\sigma_t\{A\}) = \frac{1}{nx}\sum_{\lambda}\left\{\sqrt{\frac{1}{nt-1}\sum_{t}\left(A(t,\lambda)-\bar{A}(t,\lambda)\right)^2}\right\}, \qquad (4)$$

and the variation of the zonal mean

$$\sigma_t(m_x\{A\}) = \sqrt{\frac{1}{nt-1}\sum_{t}\left(\left\{\frac{1}{nx}\sum_{\lambda}A(t,\lambda)\right\} - \overline{\left\{\frac{1}{nx}\sum_{\lambda}A(t,\lambda)\right\}}\right)^2}. \qquad (5)$$

Both proxies, characterized here, are the most prominent features of the middle atmosphere dynamics. To obtain a temporally resolved behavior of wave signals, the proxies are applied for a 48-days running window shifted by one day for each height. The integer (nx, $nt = 48\,d$) denotes the length of the sample in longitude and time, respectively.

Concerning the PW-proxy amplitudes derived from SABER data we use only nocturnal values (T_{dsc}) and normalize these by the long-term total standard deviation

$$\sigma_{tot} = \sqrt{\frac{1}{nt\cdot nx-1}\sum_{t}\sum_{\lambda}(A-\bar{A})^2} \qquad (6)$$

for each latitude and height, separately. The length of the time interval used here has the value $nt = 730$. For the analysis of PW, possible tidal effects are clearly reduced above 80 km and the increasing amplitudes of GW amplitudes with altitude are weighted by σ_{tot} to obtain a stronger picture of modulation effects by PW from the stratosphere to the lower thermosphere.

4. Validation of Planetary Wave Results

The temperature data from the MetOffice reanalysis product (0-60 km) overlap with those retrieved from SABER (30-130 km). Thus, in this section we compare PW results obtained from these two different data sets.

Figure 3 presents a height-latitude cross-section of stationary (left panel) and travelling (right panel) PW-proxies derived from MetOffice (contours) and SABER (greyscaling)

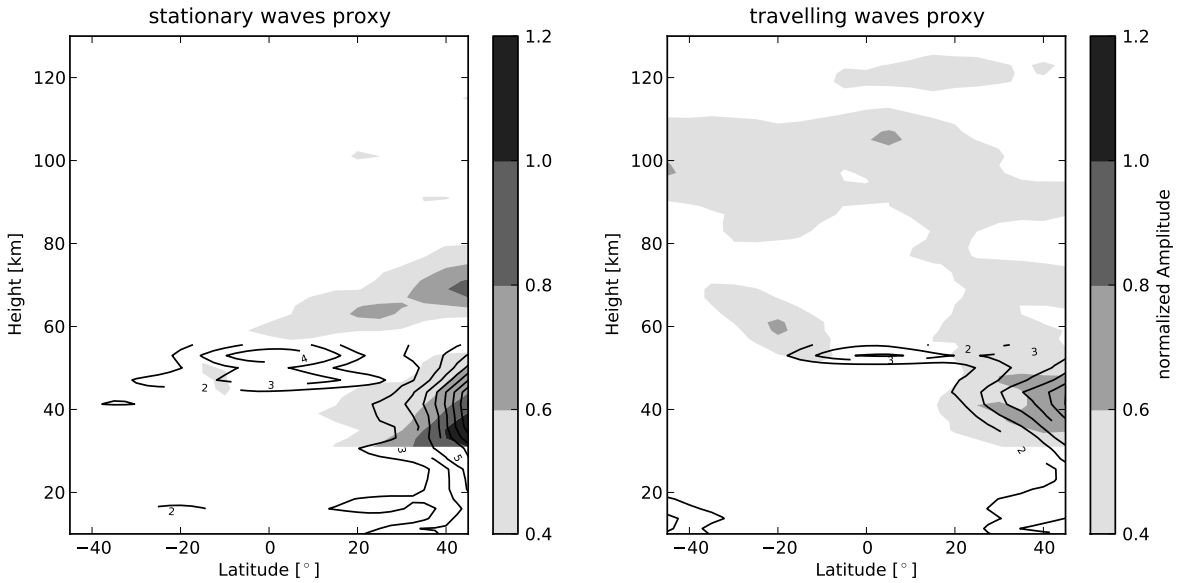

Figure 3: *Height-latitude cross-section of stationary (left panel) and travelling (right panel) wave activity applying PW-proxies to MetOffice (contours) and SABER (greyscaling) temperature data. The picture represents the averaged situation for the winter 2003/04*

temperature data. The distribution of PW activity was averaged for the winter (Dec-Jan) situation (2003/04). The PW amplitudes obtained from SABER are normalized by the total standard deviation (as described in section 3). The picture on the winter hemisphere (+45°N) is determined by stationary- and travelling PW. Using such a proxy of travelling PW both westward propagating Rossby waves and eastward wave components are collected. Between 30-60 km both data sets show a generally good agreement, however, around the equator differences occur near 50 km. We discuss this problem in the next paragraph.

The time-latitude picture at 50 km (∼1 hPa) shown in Figure 4 reveals that the signatures of the stationary component (upper panel) in MetOffice data (contours) around the equator have a semi-annual period with an amplitude of 3-4 K. This phenomenon is not visible in the SABER data (greyscaling). In Pancheva et al. (2009a) a northern hemisphere time-latitude plane of the stationary PW (SPW1, SPW2, SPW3) is presented near 40 km. Differences around the equator exist but they are smaller than 1 K. One may speculate that the reanalyses at lowlatitudes above 40 km could be questionable. Due to the decreased number of observation with height, and the forcing mechanism of the equatorial semi-annual oscillation due to equatorial waves, the reliability in the troposphere/lower stratosphere is much higher. Notwithstanding possible problems with PW analyses at equatorial regions, the PW at midlatitudes retrieved from both data sets indicate a good agreement. Due to the averaging process by fitting the satellite measurements to the 3D-grid, the SABER wave amplitudes are a little smaller (<1 K) in comparison to MetOffice.

The height-time cross-sections of PW-proxies at 45°N are presented in Figure 5. While MetOffice data are regularly produced up to 0.1 hPa (∼60 km), space based temperature

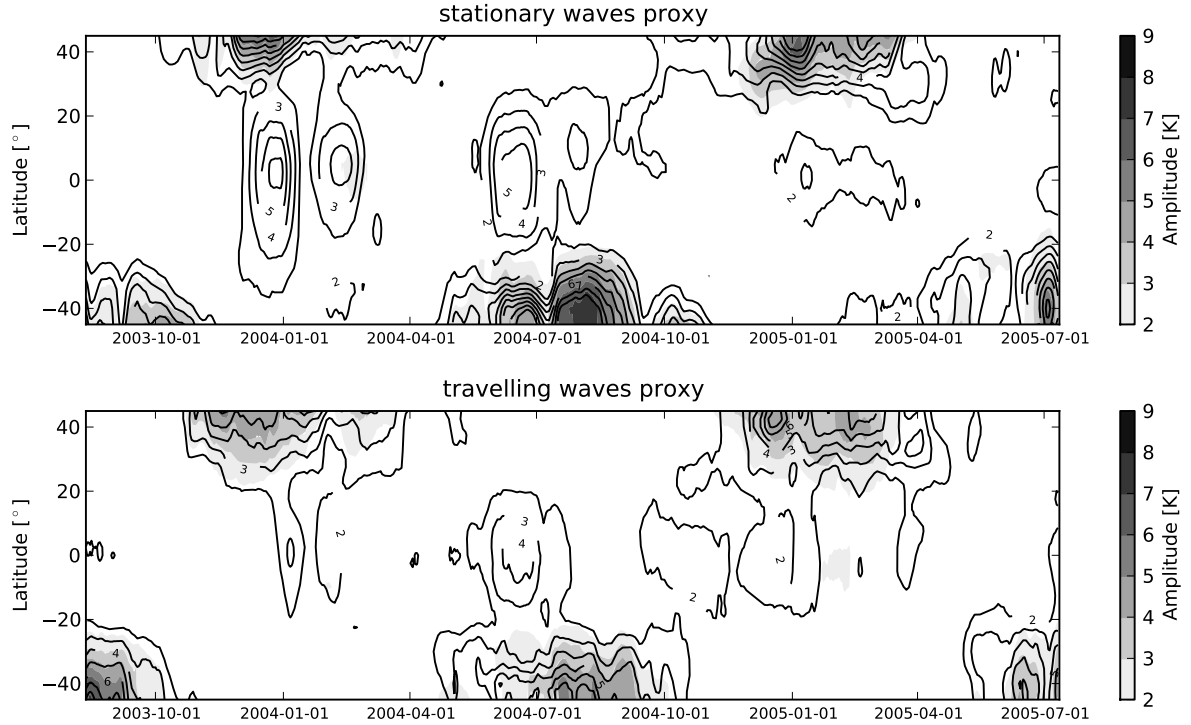

Figure 4: *Time-latitude plane at about 50km of the stationary PW-proxy (upper panel) and travelling PW-proxy (lower) derived from SABER (greyscaling) and MetOffice (contours).*

measurements including the mesosphere and lower thermosphere up to 130 km. Note, that the data above 80 km are aliased due the tidal wave amplitudes increasing with altitude. To reduce this effect the amplitudes of proxies are normalized by σ_{tot} (see section 3). The temporal and spatial structure of the stationary (upper panel) and travelling (lower panel) PW-proxy at 45°N seems consistent with the amplitude of SPW1 and long-period PW (winter 2003/04) presented in Pancheva et al. (2009a). Two maxima of the stationary wave occur around 40 km and 70 km in both cases as well as the break in January 2004 caused by major sudden stratospheric warming (SSW). Finally, from Figure 5 one can see that PW are not able to propagate directly into the lower thermosphere.

5. Modulation of GW by PW

GW, which cover a broad range of horizontal and vertical wavelengths shorter than those of PW as well as frequencies between buoyancy and inertial frequency, are considered to be able to transfer signals of stratospheric PW into the upper neutral atmosphere. Their amplitudes cause fluctuations in the thermosphere density and composition modulated by PW from below. Due to the connection of the thermosphere and ionosphere, signatures of PW then should be also visible in the ionised component.

Analogue to the previous section, PW-proxies are determined to obtain a general picture

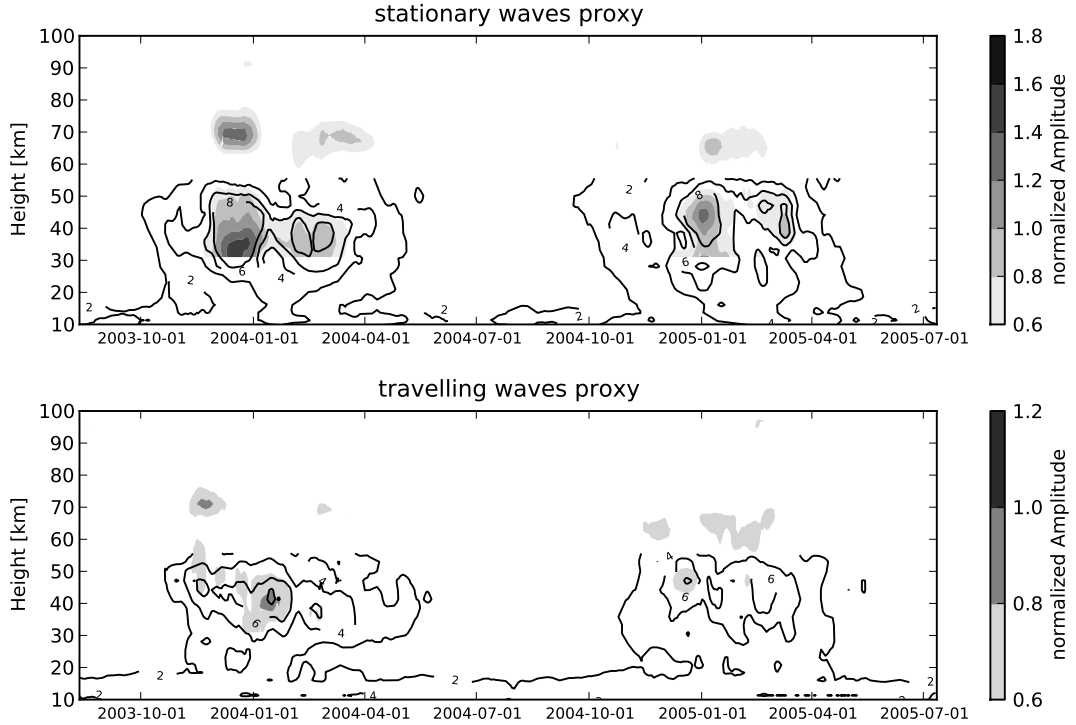

Figure 5: *Time-altitude cross-section at 45°N of the stationary PW-proxy (upper panel) and travelling PW-proxy (lower panel) derived from SABER (greyscaling) and MetOffice (contours). The PW-proxies in SABER are normalized by the total standard deviation in the time-longitude domain at each height.*

of modulation effects of GW by global scale waves such as PW. The latitude-height cross-section presented in Figure 6 shows the GW modulation by stationary (left) and travelling (right) PW for winter 2003/04 (Dec-Jan). The latitudinal distribution reveals signatures of stratospheric PW in the GW potential energy at mid-latitudes (greyscaling). At lower latitudes and in the southern hemisphere no signals of PW exist. In the mesosphere/lower thermosphere (80-130 km) a similar latitudinal structure of GW modulation by PW can be observed only for the travelling component. However, a maximum of this proxy near the summer mesopause (80 km) at 45°S is found. Figure 7 depicts the modulated GW potential energy (greyscaling) by stationary (upper panel) and travelling (lower panel) components. The magnitudes are again normalized by σ_{tot} for each altitude. The contour lines show the associated PW activity derived from MetOffice for the stationary- and travelling proxies, respectively.

In section 4 we have already shown that PW cannot propagate directly into the thermosphere, but we suppose that signatures of PW are able to be transfered from the stratosphere to the lower thermosphere indirectly by the modulation of GW. These have smaller horizontal and vertical scales than PW, which enables them to overcome the mesopause and penetrate the lower thermosphere. From Figure 7 we can conclude that especially travelling PW modulate GW at stratospheric heights and these signatures are detected,

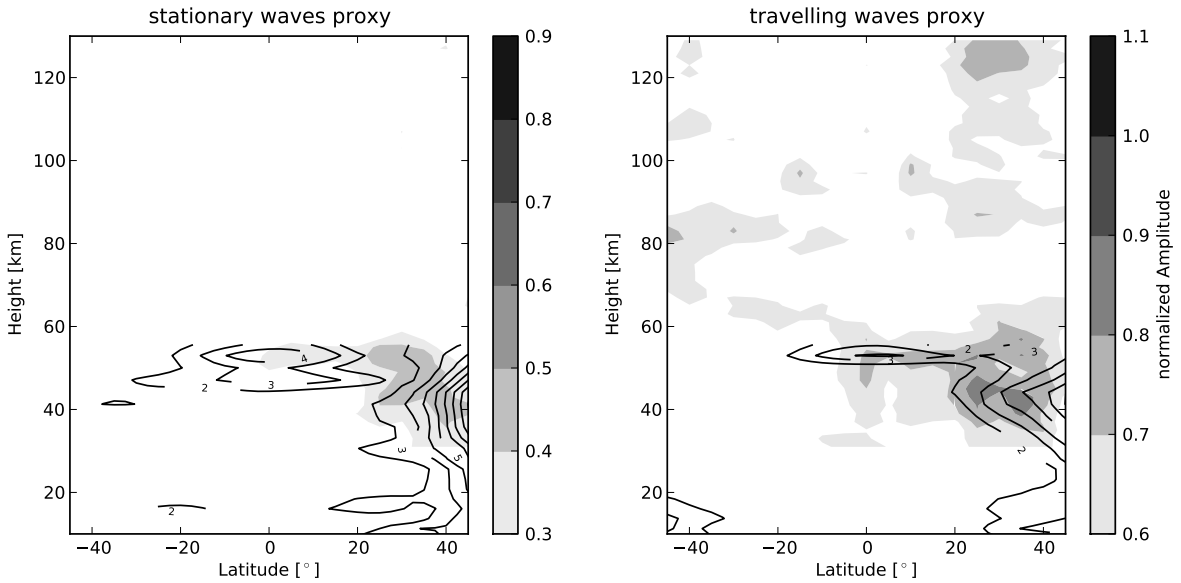

Figure 6: *Similar to Figure 3, but the normalized potential energy of GW derived from SABER (greyscaling) is shown.*

although slightly modified at 120 km similar to PW activity. In mid-winter 2003/04, we observe two maxima of travelling proxy amplitudes in GW potential energy signals during early and late winter. This behaviour is connected to SSW showing a break in the stationary proxy and the modulation of GW by travelling PW. The same structure can be observed between 90-120 km. In winter 2004/05 (without SSW), the modulation of GW is not disturbed, but the signals of GW above 90 km appear different to the stratosphere.

A special phenomenon is observed around the summer mesopause which shows a maximum of GW modulation, probably caused by in situ processes. A connection to the quasi-2-day wave (QTDW) is assumed, which maximises in summer at midlatitudes (Jacobi et al., 1997). In this connection, the low values of the normalized proxies that occur in the winter mesopause are caused by the large summer amplitudes such that the winter PW are underestimated. Thus, the signature of PW should be continuously visible by the modulation of GW.

6. Coupling between atmosphere/ionosphere

As already demonstrated in the previous section, PW may modulate GW and their signatures can propagate into the lower thermosphere almost continuously. In this section we present evidence of the indirect coupling mechanism between stratosphere travelling PW and ionospheric PWTO by an example of the modulation of GW at 45°N.

Figure 8 shows the time series of travelling PW-proxy applied to data at different heights from the stratosphere (40 km) up to the ionosphere (∼300 km). Their amplitudes are normalized and scaled in according to the corresponding height. The stratospheric PW from MetOffice data at about 40 km (thick dark line) represents the actual wave activity of the travelling components. In addition, the modulation of GW by travelling PW

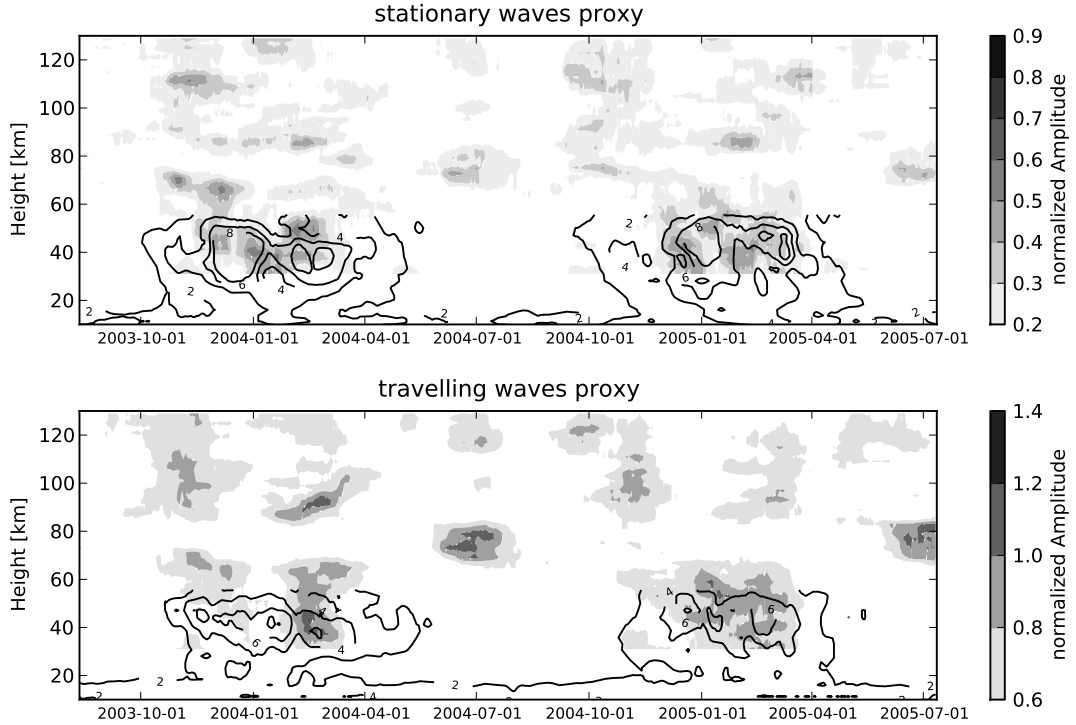

Figure 7: *Time-altitude cross-section at 45°N of GW modulation by stationary (upper panel) and travelling (lower panel) PW. The PW-proxies of GW (greyscaling) derived from SABER are normalized by the total standard deviation in comparison to PW-proxies obtained from MetOffice (contours).*

derived from SABER at 8 different heights (thin grey lines) averaged over 10 km are added from the stratosphere (30 km) to the lower thermosphere (120 km). The time series of the modulated signal reproduces the one of the PW activity especially in early and late winter 2003/04 (grey shaded). One observes a signal of PW in the stratosphere and a modulation of GW up to 120 km. At the same time signatures of PW in the ionosphere by modulation of TID (thick dotted line) and PWTO (thick dashed line) derived from TEC can be detected. We may consider this result as a supporting evidence for an indirect vertical coupling between the stratosphere and ionosphere. The situation in winter 2004/05 differs from the previous one. There is no SSW and the modulation of GW by PW follows the course of the PW activity up to 90 km relatively well. Above, the character occur slightly changed, however, a possible correspondence can be found with respect to proxies derived from ionospheric data. However, there is no clear similarity in the behaviour of the different parameters, especially in December 2004. At 120 km the GW potential energy shows a minimum while TID signatures indicate a maximum. In contrast to that, the proxy of PWTO reveals no important change. We may conclude that there is a possible coupling between PW, GW modulation, TID and PWTO, however, this coupling is intermittent and does not occur necessarily in every winter.

The summer maximum around 80 km seems to be caused by in situ processes in connection

with the QTDW. Neither stratospheric PW nor signatures of PW in the ionosphere are visible in the TID and TEC data.

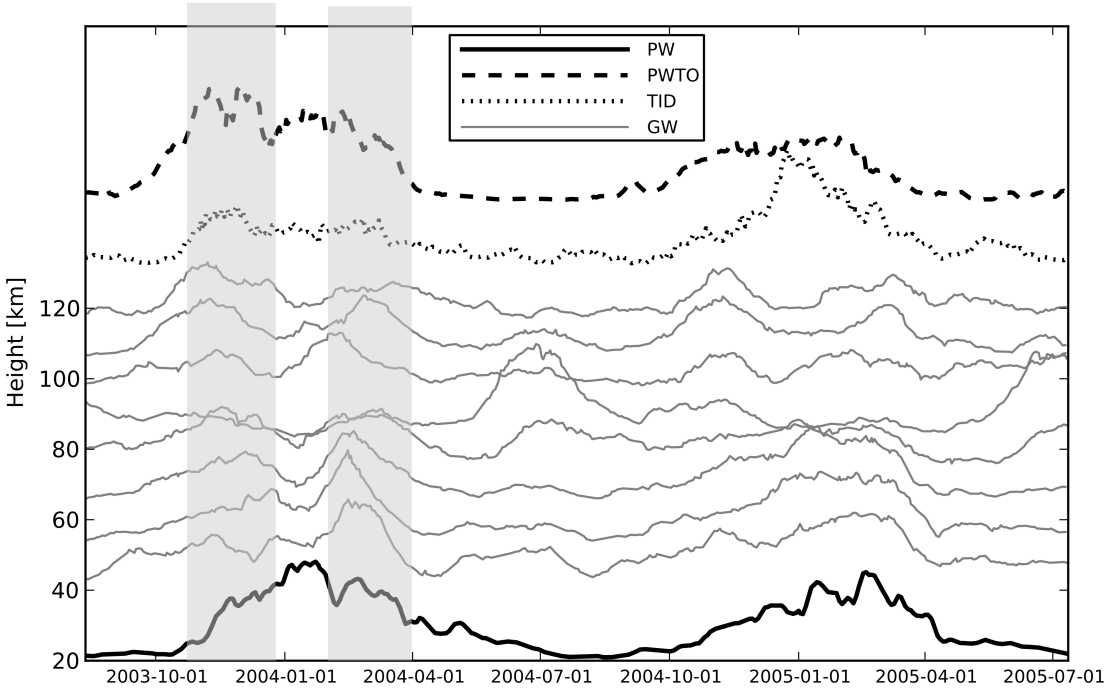

Figure 8: *Time series of travelling PW-proxies for different parameters at several heights. Starting from below: PW (thick dark line), GW (thin grey lines), TID (dotted line) and PWTO (dashed line). All amplitudes (A) are normalized by the long-term mean ($\bar{A}$) and scaled according to the corresponding height:*
$A_{PW} = 20 + 10 \cdot (A/\bar{A})$, $A_{GW} = h_z + 30 \cdot (A/\bar{A})$, $A_{TID} = 130 + 10 \cdot (A/\bar{A})$, $150 + A_{PWTO} = 10 \cdot (A/\bar{A})$

7. Conclusions

A possible connection between stratospheric PW and ionospheric PWTO by the modulation of GW potential energy derived from SABER (space-based) temperature profiles is presented in this paper using proxies of PW activity. To this end, we have used SABER temperatures and MetOffice reanalyses. At first, we have shown that PW proxies (stationary and travelling) derived from both data sets are conform at midlatitudes. Up to about 70 km the SABER data deliver reliable results of PW without aliasing effects that are, near the mesopause, caused by the sun-synchronous observation and the increasing tidal amplitudes in the upper mesosphere. However, using the normalization by σ_{tot} this influence can be reduced. The results of our analysis confirm literature results that stationary waves cannot propagate higher than about 80 km.

Furthermore, the mechanism of vertical coupling between the stratosphere and ionosphere through the modulation of GW by PW has been analysed. It could be demonstrated that during some winters GW amplitudes are modulated by PW and propagate directly upward

up to the lower thermosphere where they may cause fluctuations in density and composition. Due to the interaction between the neutral and ionised component of the upper atmosphere possible modulation effects could trigger TID and finally PWTO, which had been demonstrated by the corresponding time serie of these parameters during one winter. The mechanism of vertical coupling, which is proved for the winter seasons 2003/04 indicates promising results that stratospheric PW activity modulates GW (PW→GW) well seen in Nov. 2003, Feb. 2004 and Feb. 2005. During these periods of time GW obviously propagate directly upward into the lower thermosphere (120 km). Due to the fact that ionospheric plasma acts to a certain degree as a tracer in the neutral atmosphere, the temporally behavior between the PW-proxy derived from GW potential energy and TID signatures appears comparable (GW→TID), except for Dec. 2004.

Although, the applied method using proxies of PW delivers only a general view of such coupling mechanism, but the results manifestate the likely relation between PW and PWTO by the transmission path PW→GW→TID→PWTO.

Acknowledgments

This study was supported by Deutsche Forschungs Gemeinschaft under grant JA 836/24-1 and JA 640/5-1. Many thanks for the stratospheric reanalysis data (MetOffice) provided by the BADC and the ionospheric TEC and TID data processed by the DLR Neustrelitz. Special thanks also to the SABER team for providing the data.

References

Altadill, D., Apostolov, E. M., Jacobi, C., Mitchell, N. J., 2003: Six-day westward propagating wave in the maximum electron density of the ionosphere. Ann. Geophys., 21, 1577-1588.

Borries, C., Jakowski, N., Jacobi, Ch., Hoffmann, P., Pogoreltsev, A., 2007: Spectral analysis of planetary waves seen in the ionospheric total electron content (TEC): First results using GPS differential TEC and stratospheric reanalyses. J. Atmos. Solar.-Terr. Phys., Vol. 69, 2442-2451, doi:10.1016/j.jastp.2007.02.004.

Borries, C., Jakowski, N. and Wilken, V., 2009: Storm induced large scale TIDs observed in GPS derived TEC. Ann. Geophys., 27, 1605-1612.

Fröhlich, K., Schmidt, T., Ern, E., Preusse, P., de la Torre, A., Wickert, W., Jacobi, Ch., 2007: The global distribution of gravity wave energy in the lower stratosphere derived from GPS data and gravity wave modelling: Attempt and challenges. J. Atmos. Solar.-Terr. Phys., 69, 2238–2248.

Hayashi, Y., 1971: A General Method of Resolving Disturbances into Progressive and Retrogressive Waves by Space Fourier and Time Cross-Spectral Analyses. J. Meteor. Soc. Japan, 49, 125-128.

Hoffmann, P., Ch. Jacobi, and S. Gimeno-Garcia, 2009: Using Python language for analysing measurements from SABER instrument on TIMED satellite. Rep. Inst. Meteorol. Univ. Leipzig 45, 139-151.

Jacobi, Ch., R. Schminder and D. Kürschner, 1997: The quasi two-day wave as seen from D1 LF wind measurements over Central Europe (52°N, 15°E) at Collm, J. Atmos. Solar-Terr. Phys., 59, 1277-1286.

Laštovička, J., 2006: Forcing of the ionosphere by waves from below. J. Atmos. Solar-Terr. Phys., 68, 479-497.

Oberheide, J., Hagan, M. E., Roble, R. G., 2003: Tidal signatures and aliasing in temperature data from slowly precessing satellites. J. Geophys. Res., Vol. 108(A2), doi:10.1029/2002JA009585.

Mertens, C. J., et al., 2004: SABER observations of mesospheric temperatures and comparisons with falling sphere measurements taken during the 2002 summer MaCWAVE campaign. Geophys. Res. Lett., 31, L03105, doi:10.1029/2003GL018605 .

Pancheva, D., Mukhtarov, P., Andonov, B., Mitchell, N. J., Forbes, J. M., 2009a: Planetary waves observed by TIMED/SABER in coupling the stratosphere–mesosphere–lower thermosphere during the winter of 2003/2004: Part 1 - Comparison with the UKMO temperature. J. Atmos. Solar.-Terr. Phys., Vol. 71, 61-74,doi:10.1016/j.jastp.2008.09.016.

Pancheva, D., Mukhtarov, P., Andonov, B., Mitchell, N. J., Forbes, J. M., 2009b: Planetary waves observed by TIMED/SABER in coupling the stratosphere–mesosphere–lower thermosphere during the winter of 2003/2004: Part 2 - Altitude and latitude planetary wave structure. J. Atmos. Solar.-Terr. Phys., Vol. 71, 75-87,doi:10.1016/j.jastp.2008.09.027.

Pogoreltsev, A. I., A. A. Vlasov. K. Fröhlich, and Ch. Jacobi, 2007: Planetary waves in coupling the lower and upper atmosphere. J. Atmos. Solar-Terr. Phys. 69, 2083-2101.

Preusse, P., Dornbrack, A., Eckermann, S.D., Riese, M., Schaeler, B., Bacmeister, J.T., Broutman, D., Grossmann, K.U, 2002: Space based measurements of stratospheric mountain waves by CRISTA, 1. Sensitivity, analysis method and a case study. J. Geophys. Res., 107, 8178.

Preusse, P., Ern, M., Eckermann, S.D., Warner, C.D., Picard, R.H., Knieling, P., Krebsbach, M., Russell, J.M., Mlynczak, M.G., Mertens, C.J., Riese, M., 2006: Tropopause to mesopause gravity waves in August: measurement and modelling. J. Atmos. Solar.-Terr. Phys., 68, 1730–1751.

Tsuda, T., Nishida, M., Rocken, C., Ware, R. H, 2000: A global morphology of gravity wave activity in the stratosphere revealed by the GPS occultation data (GPS/MET). J. Geophys. Res., 105, 7257-7273.

Addresses of the Authors:

Peter Hoffmann (phoffmann@uni-leipzig.de)
Christoph Jacobi (jacobi@uni-leipzig.de)

Institute for Meteorology
University of Leipzig
Stephanstr. 3
04103 LEIPZIG